CHEMISTRY OF MATERIALS
Cite This: Chem. Mater. XXXX, XXX, XXX−XXX
Article
pubs.acs.org/cm

Influence of the Contact Area on the Current Density across Molecular Tunneling Junctions Measured with EGaIn Top-Electrodes

Philipp Rothemund,[†,‡,§] Carleen Morris Bowers,[‡] Zhigang Suo,[†,§] and George M. Whitesides*[,‡,§,∥]

[†]School of Engineering and Applied Sciences, Harvard University, 29 Oxford Street, Cambridge, Massachusetts 02138, United States
[‡]Department of Chemistry and Chemical Biology, Harvard University, 12 Oxford Street, Cambridge, Massachusetts 02138, United States
[§]Kavli Institute for Bionano Science and Technology, Harvard University, 29 Oxford Street, Cambridge, Massachusetts 02138, United States
[∥]Wyss Institute of Biologically Inspired Engineering, 60 Oxford Street, Cambridge, Massachusetts 02138, United States

Supporting Information

ABSTRACT: This paper describes the relationship between the rates of charge transport (by tunneling) across self-assembled monolayers (SAMs) in a metal/SAM//Ga_2O_3/EGaIn junction and the geometric contact area (A_g) between the conical Ga_2O_3/EGaIn top-electrode and the bottom-electrode. Measurements of current density, $J(V)$, across SAMs of decanethiolate on silver demonstrate that $J(V)$ increases with A_g when the contact area is small (A_g < 1000 μm^2), but reaches a plateau between 1000 and 4000 μm^2, where $J(0.5\ V) \approx 10^{-0.52\pm0.10}$ A/cm^2. The method used to fabricate Ga_2O_3/EGaIn electrodes generates a tip whose apex is thicker and rougher than its thin, smoother sides. When A_g is small, the Ga_2O_3/EGaIn electrode contacts the bottom-electrode principally over this rough apex and forms irreproducible areas of electrical contact. When A_g is large, the contact is through the smoother regions peripheral to the apex and is much more reproducible. Measurements of contact pressure between conical EGaIn electrodes and atomic force microscope cantilevers demonstrate that the nominal contact pressure (governed by the mechanical behavior of the oxide skin) decreases approximately inversely with the diameter of geometric contact. This self-regulation of pressure prevents damage to the SAM and makes the ratio of electrical contact area to geometric footprint approximately constant.

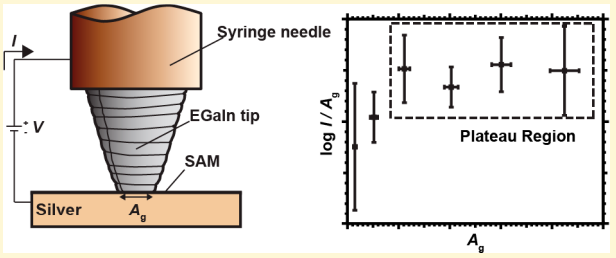

INTRODUCTION

For measurements of charge transport across thin organic films (here, self-assembled monolayers, or SAMs), we and others have used EGaIn (a eutectic alloy of gallium and indium) suspended from a syringe needle as the top-electrode (Figure 1).[1] EGaIn is a liquid metal alloy at room temperature; it forms a thin oxide skin (reported to be ∼0.7 nm on average on a quiescent film, as measured by angle-resolved X-ray photoelectron spectroscopy (XPS), but much thicker in some parts of the EGaIn junction),[2] which consists predominately of gallium oxide. For simplicity, we refer to the oxide skin as Ga_2O_3, although its composition seems to include oxygen defects and probably other materials (for example adsorbed organics) on its surface when exposed to air.[2−4] This skin allows us to shape or mold EGaIn into sharp conical tips (with a round apex of ∼50 μm radius of curvature at the apex).[2] For brevity, the community using this electrode tip refers to it as an EGaIn electrode or EGaIn tip, although it is really a Ga_2O_3/EGaIn tip.

The Ga_2O_3 layer is sufficiently electrically conducting (resistivity $\rho_{Ga_2O_3} \approx 1\ \Omega$ cm) that it does not, under normal use of the EGaIn electrode, contribute to the resistivity of a junction of the structure Met^{TS}AR//Ga_2O_3/EGaIn (where Met^{TS} is a template stripped Au or Ag bottom electrode,[5] A is an anchoring group, or atom, and R is the organic unit making up the SAM).[2,6,7] (Polarization of this electrode at potentials >1 V results in a drop in conductivity; Nijhuis et al. suggested that this drop reflects an electrochemical reaction with water and ions present in the junction.[4]) This solid film of Ga_2O_3, however, buckles and folds during fabrication of the tip, and as it is manipulated during use, and this mechanical deformation causes the surface of the electrode to be rough on the microscale. Due to the roughness of the film of Ga_2O_3 at the apex of the tip (and the substrate), the contact between the EGaIn electrode and the SAM is imperfect, and thus current flows through only a fraction of the geometric contact area (A_g, μm^2) of the junction (Figure 1). We define the area through which current flows as the effective electrical contact area (A_e, μm^2). We,[6] and Nijhuis and coworkers,[8,9] estimated the effective electrical contact area to be ∼10^{-4} the geometric

Received: August 9, 2017
Revised: December 7, 2017
Published: December 7, 2017

DOI: 10.1021/acs.chemmater.7b03384
Chem. Mater. XXXX, XXX, XXX−XXX

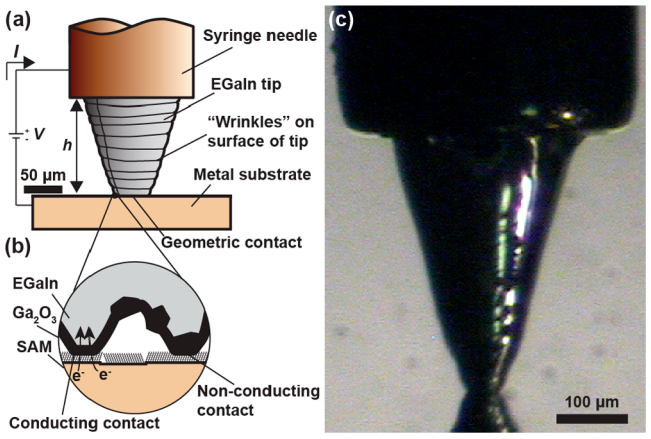

Figure 1. Schematic of a large-area tunneling junction using an EGaIn conical tip as the top-electrode. The electrical junction is established by pushing the EGaIn electrode onto a SAM bound to an ostensibly flat metal bottom-electrode. (a) Liquid EGaIn is covered with a thin, electrically conductive skin (~0.7 nm) of Ga_2O_3. This skin retains the conical shape of the tip and contributes to the contact of this top-electrode with the SAM. Wrinkling of the Ga_2O_3 skin serves as a useful qualitative indicator for compressive stress. (b) Roughness of the bottom-electrode, and the inhomogeneity and roughness of the Ga_2O_3 skin, result in a ratio of 10^4 of the apparent (geometric) contact area of the tip with the SAM to the electrically conducting contact area. The relative dimensions in panel b (or a) are not intended to be accurate; the lumps of Ga_2O_3 may be up to several μm-thick in size (we do not know their distribution in sizes).[2] (c) Image of a tunneling junction with an EGaIn conical tip (as the top-electrode) in contact with a SAM supported on Ag^{TS}.

contact area. This value, although small, is expected for two physical bodies in mechanical contact.[10]

To measure the tunneling current across a junction comprising a thin insulating layer (the SAM) and top- (Ga_2O_3/EGaIn) and bottom-electrodes, we apply a voltage (V, V), which produces a flow of electrical current ($I(V)$, A). Because the geometric contact area depends to some extent on the details of the experimental procedure used by different investigators to form the junction, we calculate the current density $J(V)$ (A/cm^2) by normalizing the measured current with the geometric contact area of the junction using eq 1, where $J(V)$ is a nominal current density because it uses the geometric contact area (A_g), and therefore does not consider the imperfect electrical contact between the EGaIn electrode and the SAM.

$$J(V) = \frac{I(V)}{A_g} \tag{1}$$

The value of $J(V)$ may depend on A_g which, in principle, might make the comparison of data measured across different junctions difficult. In practice, the values of $J(V)$ measured for a common reference compound (typically alkanethiols, which form SAMs easily on Au^{TS} or Ag^{TS}) are constant in replicate experiments within the same laboratory (we commonly observe a standard deviation of the mean of log ($J(V)$/A cm^{-2}) of $\sigma_{log} \sim 0.3$).

Reported values of $J(V)$ for the same compound across laboratories have differed by up to two orders of magnitude.[6,11−13] This variability is not important when correlating the structure of the SAM (in a group of structurally different but similar alkanethiolates) with $J(V)$ across the SAM (as is the case in the most common uses of these junctions),[6,7,14] but it is useful to understand its origin. Also, variability in the operation of junctions with light loads tends to be larger than with heavier loads. Laboratories that have measured with light contact pressure (making the plausible argument that measuring at small contact areas reduces the probability to contact a defect in the SAM[15] or that measuring with light contact pressures might avoid damage to the SAM[11]) obtain smaller values of $J(V)$ than do those who use contact pressures high enough to deform the EGaIn tip and cause a visible change in the wrinkling of the oxide skin (Video S1).[6,11,12] In this work, we systematically investigated the dependence of $J(V)$ on A_g to explain the discrepancy of the current density values measured between laboratories and determine a stable procedure.

Normal use of EGaIn electrodes does not include measuring the contact pressure when establishing a junction; instead, it relies on visual feedback from the mechanical contact to ascertain whether a small or large pressure is exerted on the junction. We, for example, relied (in our previous work with this electrode) on the wrinkling of its oxide skin (visible as a sudden change of reflection of light at the electrode close to the contact point, see Video S1) as an indication that sufficient pressure had been applied.[6] This type of visual feedback might be subjective in its interpretation or difficult to observe (wrinkling can only be observed if light reflects from the contact) and gives only qualitative information about the applied contact pressure on the tunneling-junction. Here, we present our measurements of $J(V)$ in relation to the value of A_g, which provides quantitative information on the applied contact (measurements at small pressures and areas suffer from their own types of uncertainties; see below).

To investigate the dependence of $J(V)$ on A_g using EGaIn conical tip electrodes, we measured the current density across SAMs of decanethiol ($C_{10}SH$) on Ag^{TS}.[5] We collected scans of $J(V)$ at 6 different geometric contact areas, ranging from ~150 to ~4200 μm^2. For each geometrical contact area, we formed, in total, 21 different junctions across at least 3 separate samples and collected 20 $J-V$ scans for each junction between −0.5 and 0.5 V. We fabricated a new tip for each junction to avoid the possible complication associated with contamination of the surface of the tips.

To investigate the dependence of $J(V)$ on A_g for a single conical tip-electrode, we measured the current density across a smooth (R_{MS} = 0.6 nm) film of iron oxide (~30 nm) sputtered on a p-type silicon bottom-electrode. Beginning with $A_g \sim 100$ μm^2, we increased the geometric contact area to $A_g \sim 16\,000$ μm^2 and measured the resulting values of $J(V)$. We independently studied the (nominal) contact pressure, p_n (kPa), defined here as the contact force divided by the geometric contact area of the junction, by pressing Ga_2O_3/EGaIn conical tips onto cantilevers fabricated for use in atomic force microscopes (AFM). Quantifying the deflection of the cantilever and the geometric area of the contact between the Ga_2O_3/EGaIn conical tip and the cantilever by optical microscopy allowed us to calculate p_n as a function of A_g.

The results of this study demonstrate that at small contact areas (which we define as $A_g < 1000$ μm^2), the measured current density across SAMs of $C_{10}SH$ on Ag^{TS} increases with increasing A_g. The formation of intermediate contact areas ($1000 < A_g < 4300$ μm^2), however, produced a stable plateau in current density where $J(0.5\text{ V}) = 10^{-0.52\pm0.10}$ A/cm^2. (We did not collect data for $A_g > 4300$ μm^2 because this contact area was approximately 3 times the contact area that we normally

DOI: 10.1021/acs.chemmater.7b03384
Chem. Mater. XXXX, XXX, XXX−XXX

use in current density measurements.) This stable value of current density can be used as a reference for the user to verify the application of sufficient contact force between the EGaIn top-electrode and a SAM-bound bottom-electrode, and thus ensures that $J(V)$ is independent of A_g when forming and measuring junctions.

Surprisingly, our measurement show that the nominal contact pressure decreases with increasing geometric contact area. This observation suggests that the risk of damaging the SAM is decreased when measuring J at large geometric contact areas.

BACKGROUND

Measurements of Rates of Charge Transport across SAMs. The tunneling current per unit of electrical contact area $J(V)$ across organic thin films depends on the shape and width of the tunneling barrier, the characteristics of the interfaces, and the polarity and magnitude of the applied voltage.[16,17] Assuming that changes to the average height of the tunneling barrier across a series of structurally homologous molecules of different length (e.g., *n*-alkanethiolates, $S(CH_2)_nCH_3$) can be neglected, the exponential decrease in current density, $J(V)$, across increasing film thicknesses can be approximated empirically by an equation of the form of eq 2.[16] In this equation (often called the simplified Simmons equation, although the relationship between this empirical parametrized form and the more detailed, sophisticated treatment of the Simmons equation is tenuous),[17] d (Å) is the width of the tunneling barrier, β ($Å^{-1}$) is the tunneling decay factor, and $J_0(V)$ (A/cm^2) is a parameter that can be defined theoretically when the influence of the interfaces is neglected. In practice, the physical interpretation of the parameter J_0, the extrapolation of a plot of log $J(V)$ vs d to d = 0 Å, is complicated; this parameter is not, in fact, mathematically well-defined when the properties of the interfaces are taken into account, and we therefore consider it simply as an empirical parameter obtained using eq 2.[6]

$$J(V) = J_0(V)e^{-\beta d} = J_0(V)10^{-\beta d/2.303} \quad (2)$$

Several theoretical treatments of tunneling across SAMs and other thin films predict an exponential dependence in current density on the distance between electrodes (that is, the assumed width of a rectangular tunneling barrier),[18−21] so parametrization of the dependence of the rate of tunneling as an exponential function of d is not entirely dependent on the Simmons equation.

The experimental techniques used to determine β and J_0 experimentally are categorized broadly into single-molecule and large-area junctions. Single-molecule approaches (e.g., scanning tunneling microscopy (STM),[22] break junctions,[23] and conducting-probe atomic force microscopy (CP-AFM)[24]) measure the conductance ($G = I/V$, A/V) across (when successful) one or a few molecules but suffer from limited information concerning the nature of the contacts to the metal electrodes or the geometry of the interfaces. Large-area techniques, using Ga_2O_3/EGaIn,[1] Hg,[25,26] or evaporated metals,[27] conducting polymers,[28] or graphene sheets[29] as the top-electrode, measure the tunneling current across many thousands of molecules present in a SAM (a crystalline surface of Ag contains ~14×10^6 Ag atoms per μm^2 with ~5.4×10^6 molecules of decanethiol adsorbed per μm^2).[30] The Ag^{TS} template stripped silver films (Ag^{TS}) used in our work are formed by evaporating a 400 nm-thick layer of Ag onto the surface of a Si-wafer, gluing a glass chip to the back of the film, and cleaving it from the wafer.[5] The resulting metal films are flat on the macroscale but contain both atomic-scale defects (e.g., ledges of the crystal planes) and mesoscale defects (grain boundaries, dust particles, and others).[5,31]

Reported values of β (~0.9−1.0 CH_2^{-1}) across SAMs composed of *n*-alkanethiolates ($S(CH_2)_nCH_3$) are largely in agreement across both single-molecule and large-area techniques.[6] The reported values of $J_0(V)$, however, vary by 10^6, depending on the junction.[6,7] By considering the characteristics of different experiments and applying several empirical corrections, we[6,32] and others[7,33] have estimated a value of $J_0(V)$ from different techniques for *n*-alkanethiolates on silver electrodes to be $J_0 \sim 10^6$ to 10^8 A/cm^2 at $V = \pm 0.5$ V.

Effective Electrical Contact Area between Two Electrodes in a Junction. When using solid or liquid top-electrodes and microscopically rough solid bottom-electrodes, the assumption that the entire geometric contact area is in contact, and that electrical current flows uniformly across the entire junction, is usually (and perhaps always) incorrect, and the use of eq 1 leads to an underestimation of $J(V)$.

Studies of friction indicate that when two rough solids are placed in physical contact, they touch only through small asperities on their surfaces.[10,34] The contact force, in combination with the distribution and shape of the asperities and the properties of the materials of the solids, determines the size of this microscopic contact area (A_m, μm^2). Initially (at negligibly small contact forces), contact is established through three asperities with (theoretically) atomically small contacts.[10] The applied contact force deforms the asperities, which increases the contact area between the two solids and allows additional surface asperities to come in contact. Direct measurement of A_m/A_g is difficult, but the functional dependence of A_m/A_g on the contact force can be deduced from frictional forces in combination with mechanical models (up to a constant prefactor, which depends on sample material, geometry, and roughness).[10,34,35]

When two metals are in physical contact, the stiffness of the materials prevents macroscopic deformation at the interface and thus limits the microscopic contact to a small number of asperities (tens of asperities rather than thousands). Asperities deform plastically under increasing contact load, and only ~0.1% of the geometric contact area is in microscopic contact (as estimated from electrical contact resistances).[10,36] Polymeric materials (e.g., Nylon) are softer than metals and deform macroscopically in the region of contact, allowing a larger number of surface asperities to come into contact (which in turn deform due to the contact force).[10,37] Timsit et al. investigated the ability of liquid mercury (Hg) to conform to surface asperities.[38] They poured Hg on a glass surface covered loosely with glass beads and found that Hg is not able conform to the surfaces close to the beads. A theoretical calculation indicated that its interfacial energy prevents Hg from conforming completely to asperities on a surface of a solid. The contact force from the weight of the liquid, however, leads to an increase in the microscopic contact, so that A_m can, depending on the shape and distribution of the surface asperities and the height of the liquid layer, become approximately equal to A_g.[38]

It is also an oversimplification to assume that surfaces in contact uniformly conduct electricity, while surfaces not in mechanical contact are electrically insulated. On the one hand,

DOI: 10.1021/acs.chemmater.7b03384
Chem. Mater. XXXX, XXX, XXX−XXX

the presence of contaminants (i.e., organic contaminants or dust particles), insulating layers of oxide, and defects in the SAM may insulate regions that are in mechanical contact.[10,25] On the other hand, charge is able to tunnel through thin air gaps and layers of adsorbed water, and this tunneling can lead to charge transport across regions that are formally not in mechanical (van der Waals) contact.[6,39] Electrical current therefore flows through an effective electric contact area (A_e), which is smaller than the microscopic (A_m) contact area.

The value of A_e/A_g differs across experimental techniques for measuring large-area molecular tunneling (i.e., tunneling across many molecules). You and coworkers[40] investigated the effective electrical contact in junctions with Au top-electrodes, which were patterned by nanotransfer printing (nTP) on SAMs of alkanedithiol on Au bottom-electrodes. Using this method, they fabricated junctions having Au top-electrodes of diameters D between 80 nm and 7 μm and measured the resistance across the junctions. They reported that the resistance decreased inversely proportional to the area of the junction (i.e. A_e/A_g is approximately constant) when D was less than 200 nm and greater than 1 μm. The resistance was independent of D when the diameter was between 200 nm and 1 μm (i.e. A_e/A_g decreases). When using Au electrodes with D < 200 nm, You et al. were able to fit their experimental data to the Simmons equation without a correction factor and concluded that the effective electric contact area was essentially equal to the geometric contact area. Electrodes with D > 1 μm were too rigid to adapt or conform to the roughness of the SAM at the nanoscale but sufficiently flexible to adapt macroscopically to the bottom-surface, leading to a constant ratio $A_e/A_g \sim 10^{-2}$.

We previously estimated the effective electrical contact of EGaIn conical tips to be 10^{-4} of the geometric contact area;[6] this estimation was made by comparing the current density across a film of thermally grown iron oxide using smooth Hg drops and rough EGaIn electrodes and also measuring the roughness of the SAM of alkanethiolate on a template-stripped silver surface with STM.

RESULTS AND DISCUSSION

Fabrication of EGaIn Conical Tip Electrodes and Formation of an Electrical Junction. To form a conical tip electrode (Video S1), we extruded a spherical drop of EGaIn from a syringe using a stainless-steel blunt-tip needle with a 0.13 mm inner diameter attached to a micromanipulator (Figure 2a and experimental apparatus shown in Figure S1), and pushed this drop onto a surface of bare Ag^{TS} (Figure 2b). The drop adhered to the Ag^{TS} surface. When we pulled the syringe away from the surface with the micromanipulator (~100 μm/s), the drop of EGaIn elongated (Figure 2c), and new Ga_2O_3 formed on the surface to accommodate the increase in surface area. Upon further retraction, the drop began to stretch and neck. With small (~50 μm) up and down motions, we molded the EGaIn into the shape of an hourglass with a diameter of ~50 μm in the neck (Figure 2d). We then quickly lifted the syringe to break the double cone in the necking region. A layer of Ga_2O_3 formed on the exposed surface of liquid EGaIn, thus freezing the conical shape (Figure 2e). In instances in which a filament of oxide formed at the apex (Figure S2), we discarded the tip. To form the junction, we replaced the bare Ag^{TS} substrate with a glass chip supporting an Ag^{TS} film and a SAM and lowered the syringe until the EGaIn electrode came in contact with the SAM (Figure 2f). The

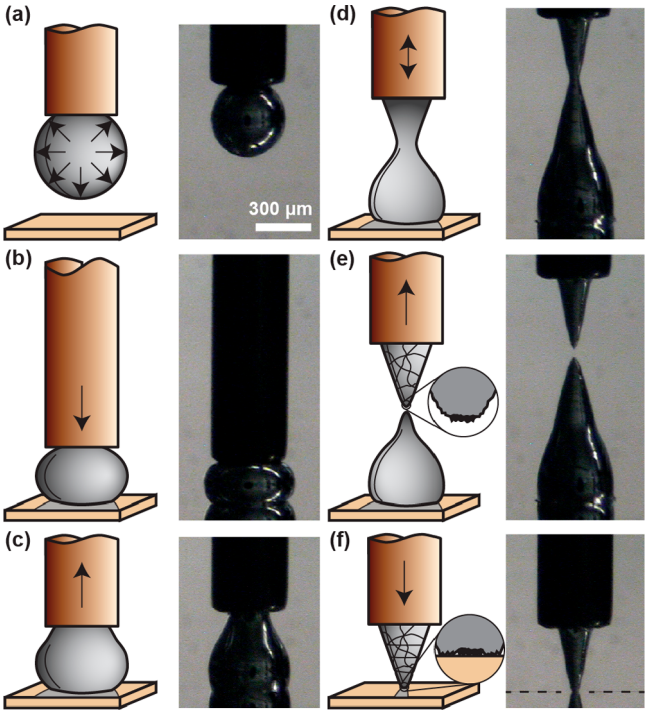

Figure 2. Fabrication of an EGaIn conical tip electrode and formation of a junction. (a) A drop of EGaIn/Ga_2O_3 is extruded from a syringe and (b) pushed on an underlying metal surface or bottom-electrode. (c) Upon retraction of the syringe from the surface, the drop elongates. (d) After the drop starts to neck, we apply small vertical motions to the syringe to shape a sharp (~50 μm) conical tip. (e) A thick layer of irregular gallium oxide forms where the EGaIn/Ga_2O_3 has ruptured. (f) A junction is formed by pushing the EGaIn tip onto a SAM until signs of mechanical deformation can be observed (deformation of the apex, wrinkling of the skin). To measure reliable data, a junction with a contact area that is larger than the region of irregular oxide has to be established.

Supporting Information contains details of the procedure used to fabricate the EGaIn electrode (Video S1).

We determined the geometric contact area between the EGaIn top-electrode and the bottom-electrode (A_g) by measuring the diameter (D, μm) of the apparent contact with optical microscopy and calculating A_g with eq 3, assuming a circular contact region between the top-electrode and the bottom-electrode.[1,25,27,28,40]

$$A_g = \frac{\pi D^2}{4} \tag{3}$$

Current Density across a Film of Iron Oxide as a Function of the Geometric Contact Area. To establish a relationship between A_g and $J(V)$ for a single EGaIn electrode, we used bottom-electrodes bearing a thin film of sputtered iron oxide (Fe_2O_3, ~30 nm thickness, $R_{MS} \sim 0.6$ nm) on n-doped silicon. We used thin films of iron oxide in our initial experiments in place of a SAM because they allowed us to increase the contact area between measurements without shorting the junction electrically.

We established initial geometric contact areas of ~100 μm^2 between the EGaIn electrode and the film of Fe_2O_3, which we determined using optical microscopy by observing the convergence of the EGaIn tip and its reflection. We measured the current of 10 linear voltage-sweeps (approximated as a series of steps of 0.05 V) between −0.5 and +0.5 V. After

DOI: 10.1021/acs.chemmater.7b03384
Chem. Mater. XXXX, XXX, XXX−XXX

forming the initial contact between the two electrodes, we increased the geometric contact area of the junction and repeated the voltage sweeps to obtain a plot of current density as a function of A_g (calculated with eq 1). We performed this experiment four times using a newly fabricated electrode in each set of experiments.

Initially, the values of $J(V)$ were irregular for all four conical tips but increased consistently until stabilizing to a plateau at $J(V = +0.5\ V) = 10^{-3.0\pm0.1}$ A/cm^2 (Figure 3). We base the

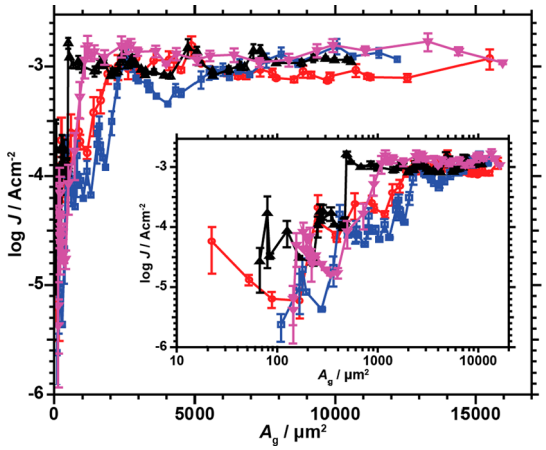

Figure 3. $J(V = +0.5\ V)$ across four junctions of the form Si/Fe_2O_3//Ga_2O_3/EGaIn. We formed a junction at an initial geometric contact area A_g < 150 μm^2 and increased it stepwise after measuring the current density for 10 voltage sweeps between −0.5 and +0.5 V. The different colors correspond to four individual junctions. The error bars show the standard deviation for the 10 voltage sweeps. The lines are meant to guide the eye. The inset shows the data with a logarithmic horizontal axis.

interpretation of this result on the structure and properties of the film of gallium oxide that forms spontaneously (in oxygen containing environments) at the apex of the conical tip during its fabrication (Figure 2, Video S1). SEM images (Figure S3) of the upward pointing (and therefore different to an unknown extent) counterpart of the conical tip on the substrate (Figure 2) show an oxide-covered, iceberg-like structure for which the oxide at the apex is rougher than that on the sides, and perhaps thicker. The rough oxide at the apex prevents conformal contact between the EGaIn electrode and the bottom-electrode. To measure reproducible and reliable values of current density across a junction with EGaIn electrodes, a user must establish a geometric contact area between the two electrodes that is larger than the region of irregular oxide at the apex of the EGaIn tip (Figure 2f).

The different EGaIn tips reached a plateau in $J(V)$ at geometric contact areas between 400 and 2200 μm^2 (this variation may depend on the size of the irregular oxide at the apex of the tip). More data are needed to obtain a statistically meaningful minimum value for A_g (that is, for the minimum geometric contact area required for reliable measurements of $J(V)$). Although the experimental procedure used here illustrated the behavior of a single tip, it differed from our standard protocol in which we fabricate a new tip for every junction. Because of the unusually long duration of the experiment, the oxide skin was exposed to atmospheric contaminants for hours as opposed to minutes. Moreover, the repeated flow of electrical current (hundreds of J−V sweeps as opposed to tens) may have changed the electrodes electrochemically. We previously observed that when we reuse a conical tip to measure three junctions, the current decreases in successive junctions.[6]

Current Densities across a SAM of $C_{10}SH$ as a Function of Contact Area. To establish a relationship between the contact area and the current density measured across an organic thin film, we measured tunneling currents across a SAM of decanethiol ($C_{10}SH$) on Ag^{TS}. This SAM is an appropriate reference sample for organic thin films because we and others have measured its electrical properties extensively.[6,14,41] The Supporting Information describes the formation of SAMs of $C_{10}SH$ on Ag^{TS} using solutions of thiol (~3 mM) dissolved in anhydrous ethanol under an atmosphere of N_2.[42] To obtain a plot of the current density as a function of the contact area, we formed junctions at 6 different contact areas and recorded the current of 20 linear voltage sweeps (approximated as a series of steps of 0.05 V) between −0.5 and +0.5 V across the junction. At each contact area, we measured 21 individual junctions (each with a newly fabricated EGaIn top-electrode) to be able to perform a meaningful statistical analysis of the data. We measured current densities at geometric contact areas starting from $A_g \sim 170$ μm^2, the smallest contact area we could achieve reproducibly, up to $A_g \sim$ 4300 μm^2 (which value corresponds to three times the geometric contact area we usually use).

The data measured across the SAM of $C_{10}SH$ shows qualitatively the same behavior as that observed with Fe_2O_3. For A_g < 1000 μm^2, the measured average current densities (J, calculated with eq 1) increase for increasing A_g and plateaus at a current density of $J(0.5\ V) = 10^{-0.52\pm0.1}$ A/cm^2 for 1000 < A_g < 4300 μm^2 (Figure 4). The height of the plateau is in good agreement with the current density measured previously across SAMs of $C_{10}SH$ on Ag^{TS}.[6,14,43]

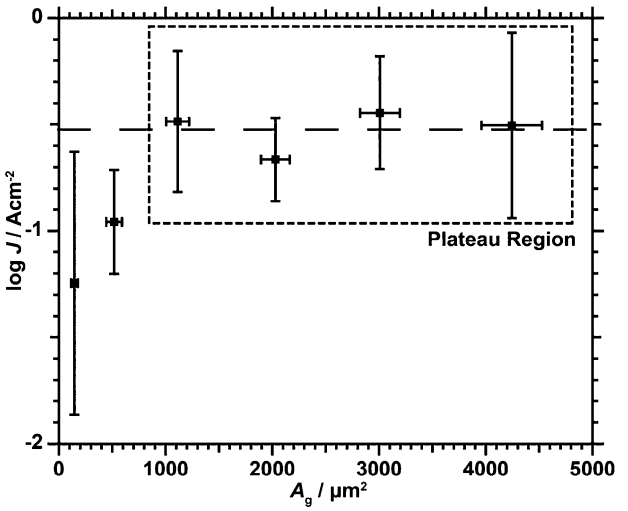

Figure 4. Measurements of current density across Ag^{TS}/S-$(CH_2)_9CH_3$//Ga_2O_3/EGaIn junctions as a function of the geometric contact area at +0.5 V. At every value of the contact area, we measured 20 J−V scans between −0.5 and 0.5 V across 21 junctions, each formed with a freshly fabricated tip. The horizontal error bars show the standard deviation of the geometric contact area of 21 junctions. The vertical error bars show the standard deviation of log J/Acm^{-2} measured at that contact area (i.e., 21 × 20 = 420 scans). While the current density increases for A_g < 1000 μm^2, it plateaus for 1000 < A_g < 4300 μm^2. The dashed line indicates height of the plateau (log J/Acm^{-2} = −0.52 ± 0.1).

DOI: 10.1021/acs.chemmater.7b03384
Chem. Mater. XXXX, XXX, XXX−XXX

Also at geometric contact areas prior to the plateau (A_g < 1000 μm^2), a fraction of the junctions (24% at A_g = 150 μm^2, 43% at A_g = 600 μm^2, Figure S4) gave current densities within a factor of 3 (±0.5 on the logarithmic scale) of the value of the plateau. The measured current densities of the other junctions were lower (up to ~2.5 orders of magnitude at A_g = 150 μm^2, up to ~1 order of magnitude at A_g = 600 μm^2, Figure S4). This observation is consistent with the measurements on iron oxide and demonstrates that some conical tips reach the plateau region earlier than others; the fewer the tips that reach the plateau, the smaller is the average value of the measured current density, and the larger is the variability from junction to junction.

This result also provides an explanation why values of $J(V)$ reported from laboratories that measure at small contact pressures (including our early work with conical EGaIn tips) are lower than the height of the plateau.[1,11,12,44] Even though the geometric contact areas at which the experiments were performed were not reported, we hypothesize that they were performed at contact areas smaller than the plateau region, and thus stable current density values were not generated.

Nijhuis and coworkers[15] also reported the observation of a plateau in current density when using an EGaIn-based tunneling junction based on a microfluidic design. (This design is different from the junction design used in the present study and does not rely on the formation of a conical tip electrode.) Specifically, they observed a plateau in current density at small geometric contact areas (A_g < 1000 μm^2) and an increase in current density at large geometric contact areas (A_g > 1000 μm^2). They attributed the increase of current at geometric contact areas beyond 1000 μm^2 to defects in the SAM. The current density J measured by Nijhuis and coworkers across as SAM of $C_{10}SH$ on Ag^{TS} is reported to be $J(V = +0.5\ V)) = 10^{-2}$ A/cm^2, which is a factor of $10^{-1.5}$ smaller than the value measured in this work and previously by us.[6,14]

Contact Pressure as a Function of Contact Area. The absolute contact forces (F, μN) between EGaIn conical tip electrodes and bottom-electrodes are small (F < 10 μN). Forces of this magnitude are difficult to measure with conventional force sensors. We used commercial silicon nitride cantilevers (Bruker Corporation; Nanoprobe DNP, k = 0.1 N/m) developed for atomic force microscopy (AFM) to measure the contact pressure exerted by a conical tip electrode onto a substrate. AFM cantilevers are linear bending beams of known spring constant k (N/m). We measured the vertical deflection of an AFM cantilever optically, while pushing an EGaIn electrode onto its end to obtain an estimate for the contact force exerted by an EGaIn electrode on a bottom-surface (Figure 5, Video S2).

We used two cameras oriented perpendicular to each other and the EGaIn electrode (Figure 5a). The front camera helped laterally align the conical tip with the cantilever (Figure 5b), whereas the side camera helped align the conical tip longitudinally (Figure 5c) and recorded the deflections (Δy, μm) and the diameter of the contact area (D) (Figure 5c). We stopped the experiment when the tip started to hang over the edge of the cantilever (Figure S5). We repeated this experiment with seven different EGaIn electrodes.

We calculated the nominal contact pressure (p_n) using eq 4 and A_g with eq 3. In using eq 3 to calculate the geometric contact area, we neglected changes of the geometric footprint from circular to elliptical shape due to tilting of the cantilever during deflection (we estimate the error due to this simplification to be smaller than 4% for the observed tilt angles up to ~15°).

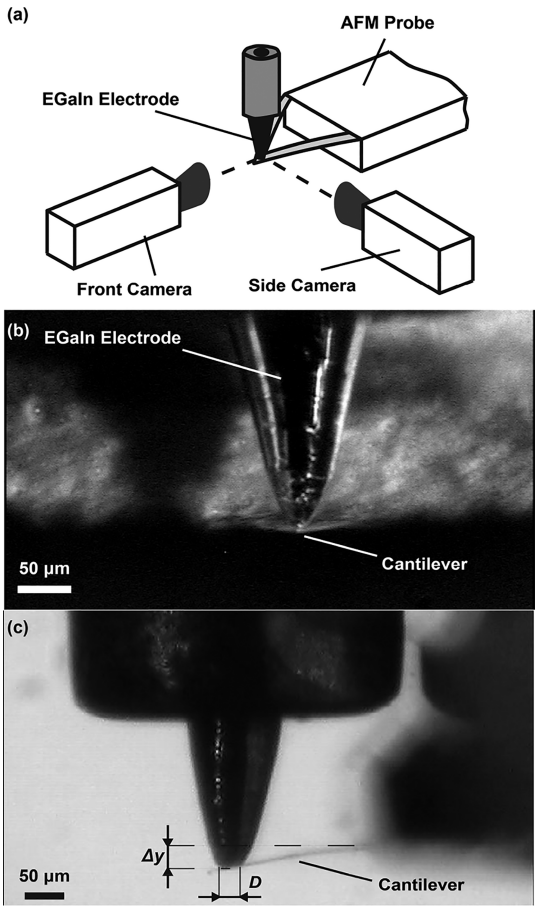

Figure 5. Measurement of contact pressure between EGaIn top-electrodes and AFM cantilevers as a function of normalized contact area. (a) An EGaIn electrode was suspended from a syringe and pressed onto a triangular AFM cantilever. The front camera is pointed to the end of the cantilever to allow aligning of the EGaIn conical tip with the camera for recording. The side camera recorded both the cantilever deflection and the diameter of the contact area. (b) Image of the AFM cantilever and EGaIn tip as seen from the front camera. (c) Image of the deflection (Δy) and diameter of the contact area (D) as seen from the side camera.

$$p_n = \frac{F}{A_g} = \frac{k\Delta y}{A_g} \quad (4)$$

For A_g < 500 μm^2, the nominal contact pressures behaved differently from tip to tip (Figure 6), possibly due to different shapes of the tip and the irregularity of the oxide at the apex. Between 500 < A_g < 2000 μm^2, the nominal contact pressure decreased with increasing geometric contact area. We could not measure at larger contact areas because all tips started to hang over the sides of the AFM cantilever.

The oxide skin present on the EGaIn electrode governs the observed decrease in contact pressure. The ~0.7 nm-thick layer of Ga_2O_3 on the sides of the conical electrode behaves like a thin membrane. It cannot sustain compressive stresses (leading to wrinkling or folding of the oxide skin) and fractures under tension when the membrane force exceeds ~0.5 N/m (creating new Ga_2O_3 from the exposed EGaIn).[3,45,46] As a result, the oxide skin does not bear load in the axial direction when the conical tip is pressed on a substrate, and the nominal contact

DOI: 10.1021/acs.chemmater.7b03384
Chem. Mater. XXXX, XXX, XXX−XXX

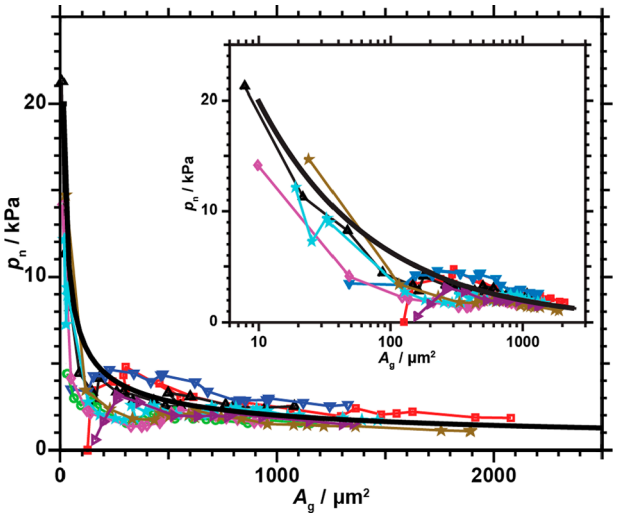

Figure 6. Measurements of the contact pressure of different conical EGaIn electrodes as a function of the geometric contact area. We measured the contact pressure by pushing conical EGaIn tips onto AFM cantilevers and calculated the contact pressure from the deflection of the cantilever and the geometric area of the contact. The colors correspond to six different EGaIn electrodes. The thick black line is a fit of a theoretical model ($p_n = K/A_g^{0.5}$, $K = 0.11 \pm 0.03$ N/m) to the data. The inset shows the data with a logarithmic horizontal axis.

pressure is equal to the pressure of the internal liquid EGaIn (see Supporting Information for details). Stresses in the oxide skin in the circumferential direction balance the pressure exerted by the liquid EGaIn on the side walls of the conical tip. Assuming that the mechanical stress in the oxide, which is required to increase the geometric contact area, is approximately constant, we developed a simple mechanical model that shows that the nominal contact pressure decreases with the diameter of the geometric contact area (i.e., the tip becomes more compliant) following an equation of the form $p_n \sim KA_g^{-0.5}$ ($K = 0.11 \pm 0.03$ N/m obtained by fitting to our experimental results; see Supporting Information for details); this curve agrees well with the experimental results (Figure 6).

CONCLUSIONS

Measurements of charge-transport with EGaIn conical tips as the top-electrode from different laboratories, and sometimes even within the same laboratory, have given values for $J(V)$ that differ. These differences have led to confusion in the comparison of data, especially for small differences in $J(V)$ for the same compound.[1,6,11,12,14] In an equation of the form $J = J_0e^{-\beta d}$ (eq 2), values of β are (usually) reproduced well between laboratories, while values of J_0 are not.

One difference in the experimental procedure between different laboratories is the size of the geometric contact area, which has been attributed to the magnitude of the pressure applied to the junction. Intuitively, higher pressure might seem likely to produce larger A_g and perhaps greater damage to the SAM by pressing the Ga_2O_3/EGaIn into the SAM.[11] Large pressure might, on the other hand, increase the mechanical stability of the junction.[6] As a result, different recommendations for the amount of contact pressure (light vs high pressure) or the size of the geometric contact area (small vs medium area) evolved.[6,11]

This work establishes that there is a plateau in $J(V)$ in an experimentally accessible region of geometric contact areas ($1000 < A_g < 4300$ μm^2), in which $J(V)$ is constant and stable. At small contact areas, $A_g < 1000$ μm^2; $J(V)$ is comparatively smaller, more variable, and area-dependent, and thus indicates that there is variability in current density measurements produced across conical tips at values of A_g smaller than those in the plateau region. We suggest performing measurements with conical EGaIn electrodes at geometric contact areas inside the plateau region because they would not only lead to better comparability of data between different laboratories and users but also eliminate the need to establish the same geometric contact for junctions within the same set of experiments.

The consistency comes from a mechanism for self-regulation in which lowering the syringe that regulates the size of the contact does not increase the nominal contact pressure, it (counterintuitively) lowers it and, unlike a previous hypothesis,[11] plausibly damages the SAM less than values at smaller contact areas. The mechanism of this autonomous regulation involves expanding the circumference of the drop against the resistive force of the Ga_2O_3 film which accommodates this expansion by fracturing and reforming. An explanation for the observed independence of $J(V)$ on the nominal contact pressure would require detailed mechanical modeling and would take into account the geometry of the asperities, the mechanical properties of the Ga_2O_3 and the bottom-electrode, and effects of surface free energy.[10,47] We have not attempted this detailed calculation.

We emphasize that no junction used to measure tunneling currents across organic molecules gives results that are free of (so far unverified) assumptions, and hence, none provides a "gold standard" to which others can be compared.[48] The best that can be done is to compare values obtained for a reference compound, an internal standard, with different junctions, and then to compare values of J for different compounds or series of compounds by normalization relative to the value of J for the internal standard obtained with that junction.

EGaIn electrodes suffer from uncertainty associated with the electrical contact area, but the simple experimental procedure and high yield of working junctions allows rapid collection of statistically meaningful data (we usually measure at least 21 junctions for each data point and use 500−1000 individual measurements of $J(V)$ curves in characterizing tunneling across a SAM). Mercury-drop electrodes suffer from some of the same uncertainties in the microscopic contact area as the EGaIn junction (although almost certainly with larger values of A_e/A_g)[38] but have smaller yields of junctions, perhaps due to amalgamation of the Hg vapor with Au or Ag making up the bottom-electrode.[25] It is difficult to interpret break-junction measurement because the nature/structure of the contact of the organic material to the electrodes is unknown.[49] Scanning probe (STM, C-AFM) measurements seem reasonably well-defined, but the measured current densities depend on the applied contact force, and extrapolating them to larger-area junctions requires some assumptions.[50] Graphene top-electrodes also do not appear to give accurate areas of electrical contact.[29] Evaporated gold top-electrodes suffer from issues associated with the unknown interface between the top-electrode and the SAM and a low yield of working junctions due to damage to the SAM during fabrication and perhaps to formation of grains and grain boundary.[51]

DOI: 10.1021/acs.chemmater.7b03384
Chem. Mater. XXXX, XXX, XXX−XXX

These comments are not intended to criticize any of these methods or even, at this stage of this field, to propose one as best; all give, we presume, values that are reproducible or replicable (depending on the experimental protocol and the system) and can be compared with other compounds measured by the same technique. Because values measured using different techniques tend, after empirical corrections, to cluster around $J_0 = 10^{6-8}$ A/cm^2, and because these values are those that emerge directly from evaporated gold and graphene, we tentatively infer that that range may include the best value of J_0 for a large area junction, but this inference requires further testing. We also note, as does Nijhuis,[9] that it may be more accurate to call the EGaIn junction a collection of small/medium-area junctions rather than a large-area junction. If $A_e/A_g \sim 10^{-4}$ and $A_g \sim 10^3$ μm^2, then A_e would incorporate $\sim 10^5$ molecules. We have no estimate of the number or distribution of areas of the regions of electrical contact, but (to choose an arbitrary but plausible number) 10^2 to 10^3 regions of equal size would suggest an average of 10^3 to 10^2 molecules per region (i.e., per contact in these small-area junctions).

■ ASSOCIATED CONTENT

Supporting Information

The Supporting Information is available free of charge on the ACS Publications website at DOI: 10.1021/acs.chemmater.7b03384.

Experimental details and materials, scanning electron micrograph of inverted Ga_2O_3/EGaIn electrode, current densities of individual junctions, derivation of mechanical model of Ga_2O_3/EGaIn electrode, and histograms of current measurements (PDF)

Video of fabrication of Ga_2O_3/EGaIn electrode (MPG)

Video of measurement of nominal contact pressure (MPG)

■ AUTHOR INFORMATION

Corresponding Author

*E-mail: gwhitesides@gmwgroup.harvard.edu.

ORCID

Zhigang Suo: 0000-0002-4068-4844

George M. Whitesides: 0000-0001-9451-2442

Notes

The authors declare no competing financial interest.

■ ACKNOWLEDGMENTS

This work was supported by a grant from the National Science Foundation (NSF, Grant CHE-1506993). P.R. and Z.S. acknowledge support from the Harvard MRSEC supported by NSF (Grant DMR 14-20570). A subcontract from Northwestern University from the United States Department of Energy (DOE, Grant DE-SC0000989) supported the salary for C.M.B for the preparation of the SAMs. Sample characterization was performed at the Center for Nanoscale Systems (CNS) at Harvard University, a member of the National Nanotechnology Infrastructure Network (NNIN), which is supported by the NSF (Grant ECS-0335765). In particular, we appreciate the assistance of Dr. Jason Tresback at CNS.

■ REFERENCES

(1) Chiechi, R. C.; Weiss, E. A.; Dickey, M. D.; Whitesides, G. M. Eutectic Gallium-Indium (EGaIn): A Moldable Liquid Metal for Electrical Characterization of Self-Assembled Monolayers. *Angew. Chem., Int. Ed.* **2008**, *47*, 142−144.

(2) Cademartiri, L.; Thuo, M. M.; Nijhuis, C. A.; Reus, W. F.; Tricard, S.; Barber, J. R.; Sodhi, R. N. S.; Brodersen, P.; Kim, C.; Chiechi, R. C.; Whitesides, G. M. Electrical Resistance of Ag^{TS}−$S(CH_2)_{n-1}CH_3$//Ga_2O_3/EGaIn Tunneling Junctions. *J. Phys. Chem. C* **2012**, *116*, 10848−10860.

(3) Dickey, M. D.; Chiechi, R. C.; Larsen, R. J.; Weiss, E. A.; Weitz, D. A.; Whitesides, G. M. Eutectic Gallium-Indium (EGaIn): A Liquid Metal Alloy for the Formation of Stable Structures in Microchannels at Room Temperature. *Adv. Funct. Mater.* **2008**, *18*, 1097−1104.

(4) Wimbush, K. S.; Fratila, R. M.; Wang, D.; Qi, D.; Liang, C.; Yuan, L.; Yakovlev, N.; Loh, K. P.; Reinhoudt, D. N.; Velders, A. H.; Nijhuis, C. A. Bias Induced Transition from an Ohmic to a Non-Ohmic Interface in Supramolecular Tunneling Junctions with Ga_2O_3/EGaIn Top Electrodes. *Nanoscale* **2014**, *6*, 11246−11258.

(5) Weiss, E. A.; Kaufman, G. K.; Kriebel, J. K.; Li, Z.; Schalek, R.; Whitesides, G. M. Si/SiO_2-Templated Formation of Ultraflat Metal Surfaces on Glass, Polymer, and Solder Supports: Their Use as Substrates for Self-Assembled Monolayers. *Langmuir* **2007**, *23*, 9686−9694.

(6) Simeone, F. C.; Yoon, H. J.; Thuo, M. M.; Barber, J. R.; Smith, B.; Whitesides, G. M. Defining the Value of Injection Current and Effective Electrical Contact Area for EGaIn-Based Molecular Tunneling Junctions. *J. Am. Chem. Soc.* **2013**, *135*, 18131−18144.

(7) Sangeeth, C. S. S.; Wan, A.; Nijhuis, C. A. Equivalent Circuits of a Self-Assembled Monolayer-Based Tunnel Junction Determined by Impedance Spectroscopy. *J. Am. Chem. Soc.* **2014**, *136*, 11134−11144.

(8) Wan, A.; Sangeeth, C. S. S.; Wang, L.; Yuan, L.; Jiang, L.; Nijhuis, C. A. Arrays of High Quality SAM-Based Junctions and Their Application in Molecular Diode Based Logic. *Nanoscale* **2015**, *7*, 19547−19556.

(9) Du, W.; Wang, T.; Chu, H.-S.; Wu, L.; Liu, R.; Sun, S.; Phua, W. K.; Wang, L.; Tomczak, N.; Nijhuis, C. A. On-Chip Molecular Electronic Plasmon Sources Based on Self-Assembled Monolayer Tunnel Junctions. Nat. *Nat. Photonics* **2016**, *10*, 274−280.

(10) Bowden, F. P.; Tabor, D. *The Friction and Lubrication of Solids*; Clarendon Press: Oxford, 1950.

(11) Sporrer, J.; Chen, J.; Wang, Z.; Thuo, M. M. Revealing the Nature of Molecule−Electrode Contact in Tunneling Junctions Using Raw Data Heat Maps. *J. Phys. Chem. Lett.* **2015**, *6*, 4952−4958.

(12) Jiang, L.; Sangeeth, C. S. S.; Yuan, L.; Thompson, D.; Nijhuis, C. A. One-Nanometer Thin Monolayers Remove the Deleterious Effect of Substrate Defects in Molecular Tunnel Junctions. *Nano Lett.* **2015**, *15*, 6643−6649.

(13) Kong, G. D.; Kim, M.; Cho, S. J.; Yoon, H. J. Gradients of Rectification: Tuning Molecular Electronic Devices by the Controlled Use of Different-Sized Diluents in Heterogeneous Self-Assembled Monolayers. *Angew. Chem., Int. Ed.* **2016**, *55*, 10307−10311.

(14) Baghbanzadeh, M.; Simeone, F. C.; Bowers, C. M.; Liao, K. C.; Thuo, M.; Baghbanzadeh, M.; Miller, M. S.; Carmichael, T. B.; Whitesides, G. M. Odd−Even Effects in Charge Transport across *n*-Alkanethiolate-Based SAMs. *J. Am. Chem. Soc.* **2014**, *136*, 16919−16925.

(15) Jiang, L.; Sangeeth, C. S. S.; Wan, A.; Vilan, A.; Nijhuis, C. A. Defect Scaling with Contact Area in EGaIn-Based Junctions: Impact on Quality, Joule Heating, and Apparent Injection Current. *J. Phys. Chem. C* **2015**, *119*, 960−969.

(16) Simmons, J. G. Generalized Formula for the Electric Tunnel Effect between Similar Electrodes Separated by a Thin Insulating Film. *J. Appl. Phys.* **1963**, *34*, 1793−1803.

(17) Vilan, A. Analyzing Molecular Current-Voltage Characteristics with the Simmons Tunneling Model: Scaling and Linearization. *J. Phys. Chem. C* **2007**, *111*, 4431−4444.

DOI: 10.1021/acs.chemmater.7b03384
Chem. Mater. XXXX, XXX, XXX−XXX

(18) Magoga, M.; Joachim, C. Conductance of Molecular Wires Connected or Bonded in Parallel. *Phys. Rev. B: Condens. Matter Mater. Phys.* **1999**, *59*, 16011−16021.
(19) Mirjani, F.; Thijssen, J. M.; Whitesides, G. M.; Ratner, M. A. Charge Transport across Insulating Self-Assembled Monolayers: Non-Equilibrium Approaches and Modeling to Relate Current and Molecular Structure. *ACS Nano* **2014**, *8*, 12428−12436.
(20) Khoo, K. H.; Chen, Y.; Li, S.; Quek, S. Y. Length Dependence of Electron Transport through Molecular Wires − a First Principles Perspective. *Phys. Chem. Chem. Phys.* **2015**, *17*, 77−96.
(21) Fagas, G.; Delaney, P.; Greer, J. C. Independent Particle Descriptions of Tunneling Using the Many-Body Quantum Transport Approach. *Phys. Rev. B: Condens. Matter Mater. Phys.* **2006**, *73*, 2413141.
(22) Fan, F. R. F.; Yang, J.; Cai, L.; Price, D. W.; Dirk, S. M.; Kosynkin, D. V.; Yao, Y.; Rawlett, A. M.; Tour, J. M.; Bard, A. J. Charge Transport through Self-Assembled Monolayers of Compounds of Interest in Molecular Electronics. *J. Am. Chem. Soc.* **2002**, *124*, 5550−5560.
(23) Xu, B.; Tao, N. J. Measurement of Single-Molecule Resistance by Repeated Formation of Molecular Junctions. *Science* **2003**, *301*, 1221−1223.
(24) Engelkes, V. B.; Beebe, J. M.; Frisbie, C. D. Length-Dependent Transport in Molecular Junctions Based on SAMs of Alkanethiols and Alkanedithiols: Effect of Metal Work Function and Applied Bias on Tunneling Efficiency and Contact Resistance. *J. Am. Chem. Soc.* **2004**, *126*, 14287−14296.
(25) Weiss, E. A.; Chiechi, R. C.; Kaufman, G. K.; Kriebel, J. K.; Li, Z.; Duati, M.; Rampi, M. A.; Whitesides, G. M. Influence of Defects on the Electrical Characteristics of Mercury-Drop Junctions: Self-Assembled Monolayers of n-Alkanethiolates on Rough and Smooth Silver. *J. Am. Chem. Soc.* **2007**, *129*, 4336−4349.
(26) Holmlin, R. E.; Haag, R.; Chabinyc, M. L.; Ismagilov, R. F.; Cohen, A. E.; Terfort, A.; Rampi, M. A.; Whitesides, G. M. Electron Transport through Thin Organic Films in Metal - Insulator - Metal Junctions Based on Self-Assembled Monolayers. *J. Am. Chem. Soc.* **2001**, *123*, 5075−5085.
(27) Kim, T. W.; Wang, G.; Lee, H.; Lee, T. Statistical Analysis of Electronic Properties of Alkanethiols in Metal−Molecule−Metal Junctions. *Nanotechnology* **2007**, *18*, 315204.
(28) Milani, F.; Grave, C.; Ferri, V.; Samorì, P.; Rampi, M. A. Ultrathin π-Conjugated Polymer Films for Simple Fabrication of Large-Area Molecular Junctions. *ChemPhysChem* **2007**, *8*, 515−518.
(29) Wang, G.; Kim, Y.; Choe, M.; Kim, T. W.; Lee, T. A New Approach for Molecular Electronic Junctions with a Multilayer Graphene Electrode. *Adv. Mater.* **2011**, *23*, 755−760.
(30) Dhirani, A.; Hines, M. A.; Fisher, A. J.; Ismail, O.; Guyot-Sionnest, P. Structure of Self-Assembled Decanethiol on Ag (111): A Molecular Resolution Scanning Tunneling Microscopy Study. *Langmuir* **1995**, *11*, 2609−2614.
(31) Miller, M. S.; Ferrato, M. A.; Niec, A.; Biesinger, M. C.; Carmichael, T. B. Ultrasmooth Gold Surfaces Prepared by Chemical Mechanical Polishing for Applications in Nanoscience. *Langmuir* **2014**, *30*, 14171−14178.
(32) Nijhuis, C. A.; Reus, W. F.; Barber, J. R.; Whitesides, G. M. Comparison of SAM-Based Junctions with Ga_2O_3/EGaIn Top Electrodes to Other Large-Area Tunneling Junctions. *J. Phys. Chem. C* **2012**, *116*, 14139−14150.
(33) Wang, G.; Kim, T. W.; Lee, H.; Lee, T. Influence of Metal-Molecule Contacts on Decay Coefficients and Specific Contact Resistances in Molecular Junctions. *Phys. Rev. B: Condens. Matter Mater. Phys.* **2007**, *76*, 205320.
(34) Persson, B. N. J.; Albohr, O.; Tartaglino, U.; Volokitin, A. I.; Tosatti, E. On the Nature of Surface Roughness with Application to Contact Mechanics, Sealing, Rubber Friction and Adhesion. *J. Phys.: Condens. Matter* **2005**, *17*, R1−R62.
(35) Greenwood, J. A.; Williamson, J. B. P. Contact of Nominally Flat Surfaces. *Proc. R. Soc. London, Ser. A* **1966**, *295*, 300−319.
(36) Moore, A. J. W. Deformation of Metals in Static and in Sliding Contact. *Proc. R. Soc. London, Ser. A* **1948**, *195*, 231−244.
(37) Archard, J. F. Elastic Deformation and the Laws of Friction. *Proc. R. Soc. London, Ser. A* **1957**, *243*, 190−205.
(38) Timsit, R. S. Electrical Contact Resistance: Properties of Stationary Interfaces. *IEEE Trans. Compon. Packag. Technol.* **1999**, *22*, 85−98.
(39) Hahn, J. R.; Hong, Y. A.; Kang, H. Electron Tunneling across an Interfacial Water Layer inside an STM Junction: Tunneling Distance, Barrier Height and Water Polarization Effect. *Appl. Phys. A: Mater. Sci. Process.* **1998**, *66*, S467−S472.
(40) Niskala, J. R.; Rice, W. C.; Bruce, R. C.; Merkel, T. J.; Tsui, F.; You, W. Tunneling Characteristics of Au-Alkanedithiol-Au Junctions Formed via Nanotransfer Printing (nTP). *J. Am. Chem. Soc.* **2012**, *134*, 12072−12082.
(41) Bowers, C. M.; Liao, K. C.; Zaba, T.; Rappoport, D.; Baghbanzadeh, M.; Breiten, B.; Krzykawska, A.; Cyganik, P.; Whitesides, G. M. Characterizing the Metal-SAM Interface in Tunneling Junctions. *ACS Nano* **2015**, *9*, 1471−1477.
(42) Love, J. C.; Estroff, L. A.; Kriebel, J. K.; Nuzzo, R. G.; Whitesides, G. M. Self-Assembled Monolayers of Thiolates on Metals as a Form of Nanotechnology. *Chem. Rev.* **2005**, *105*, 1103−1169.
(43) Bowers, C. M.; Liao, K. C.; Yoon, H. J.; Rappoport, D.; Baghbanzadeh, M.; Simeone, F. C.; Whitesides, G. M. Introducing Ionic and/or Hydrogen Bonds into the SAM//Ga_2O_3 Top- Interface of $Ag^{TS}/S(CH_2)_nT//Ga_2O_3$/EGa. *Nano Lett.* **2014**, *14*, 3521−3526.
(44) Thuo, M. M.; Reus, W. F.; Nijhuis, C. A.; Barber, J. R.; Kim, C.; Schulz, M. D.; Whitesides, G. M. Odd-Even Effects in Charge Transport across Self-Assembled Monolayers. *J. Am. Chem. Soc.* **2011**, *133*, 2962−2975.
(45) Mansfield, E. H. Tension Field Theory, a New Approach Which Shows Its Duality with Inextensional Theory. In *Applied Mechanics; Proceedings of the Twelfth International Congress of Applied Mechanics, Stanford University*, August 26−31, 1968; Hetényi, M., Vincenti, W. G., Eds.; Springer: Berlin, Heidelberg, 1969; pp 305−320.
(46) Reissner, E. On Tension Field Theory. *Proc. 5th Int. Congr. Appl. Mech. Harvard Univ. MIT* **1938**, 88−92.
(47) Liao, K. C.; Bowers, C. M.; Yoon, H. J.; Whitesides, G. M. Fluorination, and Tunneling across Molecular Junctions. *J. Am. Chem. Soc.* **2015**, *137*, 3852−3858.
(48) McCreery, R. L.; Bergren, A. J. Progress with Molecular Electronic Junctions: Meeting Experimental Challenges in Design and Fabrication. *Adv. Mater.* **2009**, *21*, 4303−4322.
(49) Vonlanthen, D.; Mishchenko, A.; Elbing, M.; Neuburger, M.; Wandlowski, T.; Mayor, M. Chemically Controlled Conductivity: Torsion-Angle Dependence in a Single-Molecule Biphenyldithiol Junction. *Angew. Chem., Int. Ed.* **2009**, *48*, 8886−8890.
(50) Wold, D. J.; Haag, R.; Rampi, M. A.; Frisbie, C. D. Distance Dependence of Electron Tunneling through Self-Assembled Monolayers Measured by Conducting Probe Atomic Force Microscopy: Unsaturated versus Saturated Molecular Junctions. *J. Phys. Chem. B* **2002**, *106*, 2813−2816.
(51) Kronemeijer, A. J.; Huisman, E. H.; Akkerman, H. B.; Goossens, A. M.; Katsouras, I.; Van Hal, P. A.; Geuns, T. C. T.; Van Der Molen, S. J.; Blom, P. W. M.; De Leeuw, D. M. Electrical Characteristics of Conjugated Self-Assembled Monolayers in Large-Area Molecular Junctions. *Appl. Phys. Lett.* **2010**, *97*, 173302.

DOI: 10.1021/acs.chemmater.7b03384
Chem. Mater. XXXX, XXX, XXX−XXX